

Formation and physical properties of Fe-based bulk metallic glasses with Ni addition

S. Lesz^{a,*}, P. Kwapuliński^b, R. Nowosielski^a

^a Division of Nanocrystalline and Functional Materials and Sustainable Pro-ecological Technologies, Institute of Engineering Materials and Biomaterials, Silesian University of Technology, ul. Konarskiego 18a, 44-100 Gliwice, Poland

^b Institute of Materials Science, University of Silesia, ul. Bankowa 12, 40-007 Katowice, Poland

* Corresponding author: E-mail address: sabina.lesz@polsl.pl

Received 27.06.2008; published in revised form 01.11.2008

Properties

ABSTRACT

Purpose: The main aim of the paper was investigations of formation and changes of physical properties (magnetic properties and microhardness) of Fe based bulk metallic glasses (BMGs) with Ni addition.

Design/methodology/approach: The following experimental techniques were used: transmission electron microscopy (TEM), scanning electron microscopy (SEM) and X-ray diffraction (XRD) phase analysis method to test the structure, electrical resistivity in situ measurements (four-point probe), measurements of magnetic properties, microhardness of investigated ribbons was determined by Vickers method.

Findings: The structural studies revealed an amorphous structure for the ribbons with thicknesses up to 0.27 mm, regardless of their thickness.

Research limitations/implications: More investigations for example Mössbauer spectrometry have to be conducted on different thickness of ribbons in order to confirm conclusions contained in the work.

Practical implications: According to the results presented in the present paper the examined Fe-based bulk glassy alloys with Ni addition as a soft ferromagnetic material may be utilized in construction of magnetic cores such as choke coils, common mode and noise filter and is of great technological interest.

Originality/value: The originality of the paper are examinations of changes of structure and physical properties on cross section and on surface of ribbons.

Keywords: Amorphous materials; Magnetic properties; Mechanical properties; XRD method; TEM; SEM; Fracture morphology

1. Introduction

Development of Fe-based bulk metallic glasses (BMGs) with good soft magnetic materials has become more and more important in the materials science field. It is well recognized that the low glass-forming ability (GFA) of Fe-based alloys has

limited the potential of using them as engineering materials. For this reason extensive efforts have been carried out to improve the GFA of metallic materials and understand the mechanism of effects of various factors on the formation, crystallization, thermal stability and property of BMGs [1-6].

For the preparation of Fe-based BMG, Fe₈₀B₂₀ is often used as the starting alloy. Further the Nb metal with high melting

temperature was addition. The addition of small amounts of Nb to (Fe,Co,Ni)-(B,Si) alloys is effective for the increase in GFA through the increase in the stability of supercooled liquid (SL) against crystallization [3]. The addition of 4 at. % Nb was found to be very effective in improving the GFA of Fe- and Co- based glassy alloys [7].

As BMGs can be produced by adding four and fifth elements to the basic ternary alloys the small amounts of elements such Si and Ni was added. A Ni addition can significantly enhance the soft magnetic properties of Fe-based glass forming alloys without deteriorating their high GFA. Metalloid elements of Si and B play crucial role in the formation of the BMGs, have effect on the GFA, thermal stability, crystallization and properties of the BMGs. These materials have a strong affinity with conventional BMGs base elements such Fe and rare earth elements, i.e. they have large negative heat of mixing with these base elements. The metalloid elements would result in crystallization and degrade the GFA of the BMGs, but on the other hand, due to the small atomic size of Si and B atoms, the proper addition can tighten the alloy structure and then stabilize the alloy against crystallization [3].

The Fe-Co based glassy alloys exhibit good soft magnetic properties, i.e., high saturation magnetization (0.8-1.3 T) and low coercivity (1-2.5 A/m) [3]. The magnetic properties of these alloys are dependent on Ni and Fe contents. The decrease of coercivity (H_c) with increasing Co content has been recognized to originate from the reduction of saturation magnetostriction [3]. The coercivity is proportional to the ratio of saturation magnetostriction (λ_s) to saturation magnetization (J_s), i.e., $H_c \sim \Delta V \times \sqrt{\rho_d} (\lambda_s / J_s)$ [8] and the slope is related to the volume (ΔV) and density (ρ_d) of internal defects in the glassy structure [8-10]. The Fe-Co based glassy alloys due to a unique properties have been commercialized in the following application fields: precision mould material, precision imprint material, precision sensor material, precision machinery material, surface coating material, cutting tool material, shot penning material, fuel cell separator material and so forth [1, 2, 11, 12]. The formation of BMGs by use of the science and technology of SL are started about 20 years ago and the new research field on the basis of this concept is believed to become more and more important in the near future.

2. Material ve method

2.1. Test material

Investigations were carried out on amorphous ribbons with compositions of $[(Fe_{0.6}Co_{0.3}Ni_{0.1})_{0.75}B_{0.2}Si_{0.05}]_{96}Nb_4$. The Fe-based master alloy ingots with compositions of $[(Fe_{0.6}Co_{0.3}Ni_{0.1})_{0.75}B_{0.2}Si_{0.05}]_{96}Nb_4$ were prepared by arc melting the mixtures of the Fe-B, Fe-Nb, Fe-Si starting alloys and pure Fe, Co, Ni metals in an argon atmosphere. The $Fe_{43}Co_{22}Ni_7B_{19}Si_5Nb_4$ alloy compositions represent nominal atomic percentages. Ribbons with thickness of 0.07 and 0.27 mm and width of 2.3 mm were prepared by the single copper roller melt spinning method. The master alloy was melted in a quartz crucible using an induction coil and pushed thereafter on a copper wheel by applying an ejection pressure of about 200 mBar.

2.2. Methodology

The microstructure of the ribbons was examined by X-ray diffraction (XRD), TEM and SEM method. The X-ray method has been performed by the use of diffractometer X-Pert PRO MP with filtered Co-K α radiation.

In order to conduct structural study, the electron microscope TESLA BS 540 in the range of 24000 \times to 66000 \times magnitude was used.

The morphology of fracture surfaces after decohesion was observed in scanning electron microscope ZEISS SUPRA 25.

The measurements of magnetic permeability μ_t (at force $H \approx 0.5$ A/m and frequency $f \approx 1$ kHz) and the intensity $\Delta\mu/\mu(t_1)$ ($\Delta\mu = \mu(t_1=30$ s) - $\mu(t_2=1800$ s)), where μ is the initial magnetic permeability measured at time t after demagnetization, have been done. For samples, the relative magnetic permeability (Maxwell-Wien bridge, frequency 1 kHz, magnetic field 0.5 A/m) at room temperature were obtained. The investigations of magnetic after effect of ribbons were performed with the use of automatic device for measurements magnetic permeability [13]. The saturation magnetization $M(T)$ was measured in situ with heating rates 5 K/min by use magnetic balance. The family of magnetization curves $M(T)$ normalized to the value at 300 K and the corresponding dM/dT curves were presented. The Curie temperature T_C is determined from the condition $dM/dT = \text{minimum}$ [9-11].

Kinetics of the crystallization process was examined by applying electrical resistivity $\rho(T)$ (four point probe). The crystallization temperature T_x of the crystallization process from the normalized isochronal resistivity curves were determined for the ribbons with thickness of 0.07 mm. The temperature T_x can be obtained from the condition $d\rho/dT=0$ [9, 10].

Microhardness was measured with a use of the Vickers hardness tester PMT-3 under a load of 49 N (50 G) [12]. The microhardness was measured on the shining surface of ribbons according to pattern presented in Fig. 1.

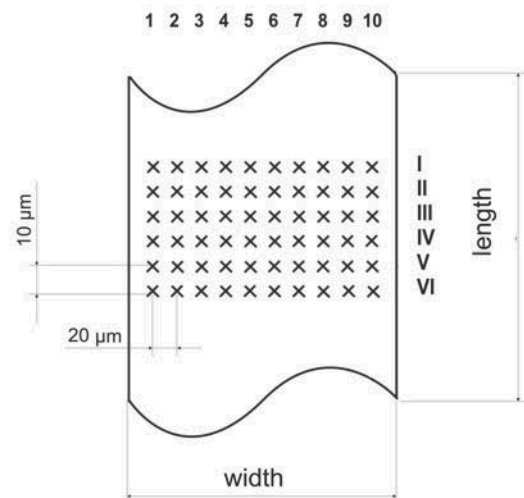


Fig. 1. The pattern of microhardness measurements

3. Results and discussion

It was found from the obtained results of structural studies performed by X-ray diffraction, transmission electron microscopy (TEM), that in as quenched state the structure of the ribbons with thickness of both 0.07 mm and 0.27 mm of $\text{Fe}_{43}\text{Co}_{22}\text{Ni}_7\text{B}_{19}\text{Si}_5\text{Nb}_4$ alloy consists of amorphous phase (Figs. 1, 2, 3). The X-ray tests prove that the structure of the both of ribbons of $\text{Fe}_{43}\text{Co}_{22}\text{Ni}_7\text{B}_{19}\text{Si}_5\text{Nb}_4$ alloy at as quenched state is amorphous, which is seen on the diffraction pattern in the form of a broad-angle peak originating from amorphous phase (Fig. 1). Obtained results of structural studies performed by X-ray diffraction are corresponding with the HRTEM micrograph (Figs. 2, 3).

The results of magnetic properties measurements, the Curie temperature T_C and the crystallization temperature of the investigated ribbons of $\text{Fe}_{43}\text{Co}_{22}\text{Ni}_7\text{B}_{19}\text{Si}_5\text{Nb}_4$ alloys have been presented in the Table 1. The value of Curie temperature is similar for $\text{Fe}_{43}\text{Co}_{22}\text{Ni}_7\text{B}_{19}\text{Si}_5\text{Nb}_4$ ribbons with thickness of 0.07 mm and 0.27 mm and is equal 529 K and 537 K, respectively (Fig. 4 a, b).

Basing on normalized isochronous curves of electric resistivity ρ as function of temperature T it was found that crystallization temperatures T_x of $\text{Fe}_{43}\text{Co}_{22}\text{Ni}_7\text{B}_{19}\text{Si}_5\text{Nb}_4$ ribbons with thickness of 0.07 mm is equal $T_x = 800$ K (Fig. 5).

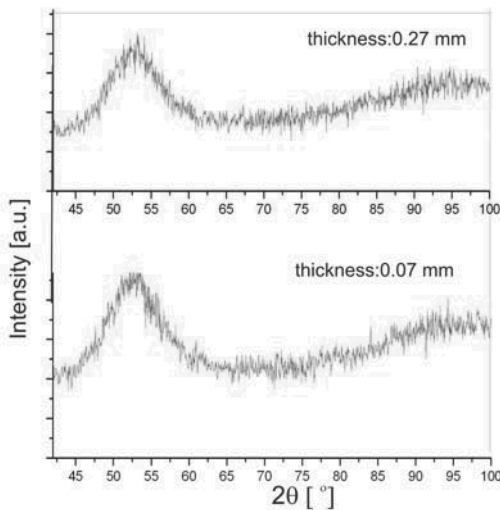


Fig. 1. X-ray diffraction pattern of $\text{Fe}_{43}\text{Co}_{22}\text{Ni}_7\text{B}_{19}\text{Si}_5\text{Nb}_4$ ribbons with thickness of 0.07 mm and 0.27 mm

Table 1. Magnetic properties (H_c - coercivity, μ_i - initial magnetic permeability, $\Delta\mu/\mu$ - magnetic after effects) and thermal stability (T_C - Curie temperature, T_x - crystallization temperature) of $\text{Fe}_{43}\text{Co}_{22}\text{Ni}_7\text{B}_{19}\text{Si}_5\text{Nb}_4$ ribbons with thickness of 0.07 mm and 0.27 mm

Thickness of ribbons	Magnetic properties			Thermal stability	
	μ_i	$\Delta\mu/\mu$ [%]	H_c [A/m]	T_C [K]	T_x [K]
0.07	1600	4.5	4.0	529	800
0.27	500	8.0	4.8	537	-

The detailed analysis of data of magnetic properties i.e. μ_i and H_c allow to classify the alloy in as quenched state as a soft magnetic material. (Table 1). The ribbons with thickness of 0.07 mm have better magnetic properties ($H_c=4.0$ A/m, $\mu_i=1600$, $\Delta\mu/\mu=4.5$, Table 1) than ribbons with thickness of 0.27 mm ($H_c=4.8$ A/m, $\mu_i=500$, $\Delta\mu/\mu=8.0$, Table 1) of $\text{Fe}_{43}\text{Co}_{22}\text{Ni}_7\text{B}_{19}\text{Si}_5\text{Nb}_4$ alloy. The thinner ribbons have better magnetic properties, what suggest that the casting conditions have influence on microvoids content and thereby on magnetic properties. These excellent magnetic properties and high value of temperature of crystallization ($T_x=800$ K- Fig. 5, Table 1) lead us to expect that the Fe-based amorphous alloy could be used as a new engineering and functional material intended for parts of inductive components. The microvoids content is often examined using magnetic after effects ($\Delta\mu/\mu$) measurements. The value of $\Delta\mu/\mu$ increases with increasing of microvoids in materials [6, 9, 10]. The obtained values of H_c and T_C of the ribbons with thickness of 0.07 mm of $\text{Fe}_{43}\text{Co}_{22}\text{Ni}_7\text{B}_{19}\text{Si}_5\text{Nb}_4$ alloy are similar than in other alloys with the similar chemical composition investigated by [12] whose results for $[(\text{Fe}_{0.6}\text{Co}_{0.3}\text{Ni}_{0.1})_{0.75}\text{B}_{0.2}\text{Si}_{0.05}]_{96}\text{Nb}_4$ and $[(\text{Fe}_{0.6}\text{Co}_{0.1}\text{Ni}_{0.3})_{0.75}\text{B}_{0.2}\text{Si}_{0.05}]_{96}\text{Nb}_4$ alloys as follows: $H_c=2$ A/m, $T_C=643$ K and $H_c=2.5$ A/m, $T_C=554$ K, respectively. Results of microhardness experiments of $\text{Fe}_{43}\text{Co}_{22}\text{Ni}_7\text{B}_{19}\text{Si}_5\text{Nb}_4$ ribbons with thickness of 0.07 mm and 0.27 mm are presented in Tables 2 and 3, respectively.

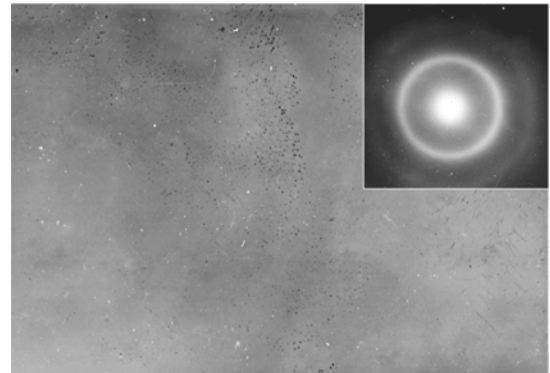


Fig. 2. TEM micrograph of $\text{Fe}_{43}\text{Co}_{22}\text{Ni}_7\text{B}_{19}\text{Si}_5\text{Nb}_4$ ribbons with thickness of 0.07 mm in as quenched state. Mag= 66000x

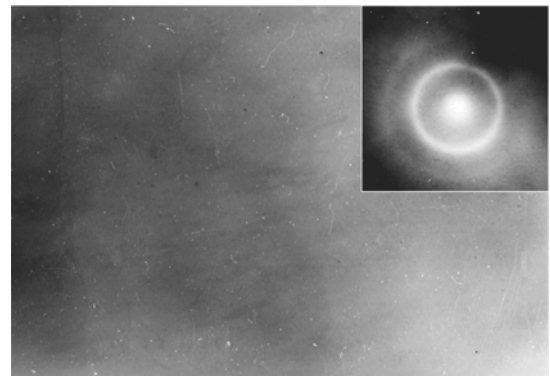


Fig. 3. TEM micrograph of $\text{Fe}_{43}\text{Co}_{22}\text{Ni}_7\text{B}_{19}\text{Si}_5\text{Nb}_4$ ribbons with thickness of 0.27 mm in as quenched state. Mag= 24000x

The results of microhardness measurements points to changeable microhardness of $\text{Fe}_{43}\text{Co}_{22}\text{Ni}_7\text{B}_{19}\text{Si}_5\text{Nb}_4$ ribbons with thickness of 0.07 mm and 0.27 mm depended on place of measurements. Microhardness varies between 1049-1648 H_v on the margin of ribbons and 927-1413 H_v in centre of $\text{Fe}_{43}\text{Co}_{22}\text{Ni}_7\text{B}_{19}\text{Si}_5\text{Nb}_4$ ribbons with thickness of 0.07 mm (Table 2). Similar microhardness varies between 874-1049 H_v on the margin of ribbons and 780-1197 H_v in centre of ribbons (Table 3).

These differences may suggest that process of solidification of amorphous ribbons is different in centre and on the margin and is

connected with cooling rate of ribbons during casting. The results of microhardness of ribbons are in agreement with findings in [12] (1240 H_v).

The significant changes of fracture morphology of $\text{Fe}_{43}\text{Co}_{22}\text{Ni}_7\text{B}_{19}\text{Si}_5\text{Nb}_4$ ribbons with thickness of both 0.07 mm and 0.27 mm after decohesion are corresponding to the observed microhardness changes. Morphology is changing from smooth fracture inside with narrow dense veins network in surface having contact with the copper roller during casting to few veins network in surface freely solidified (shining surface) (Figs. 6, 7, 8).

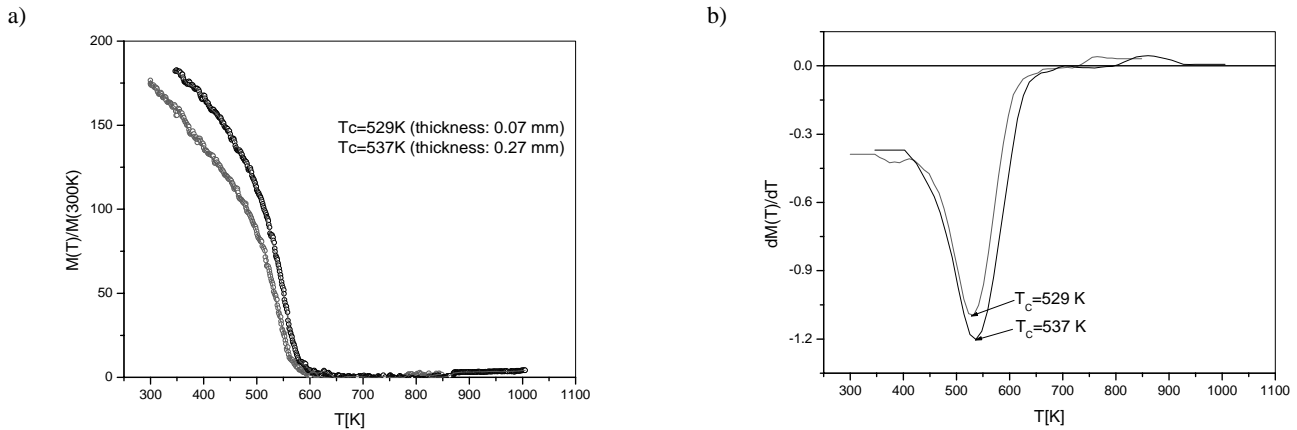


Fig. 4. Normalized magnetization versus temperature T of $\text{Fe}_{43}\text{Co}_{22}\text{Ni}_7\text{B}_{19}\text{Si}_5\text{Nb}_4$ ribbons with thickness of 0.07 mm and 0.27 mm (a) and (b) - dM/dT curves for the data presented in (a)

Table 2.

Results of microhardness H_v experiments of $\text{Fe}_{43}\text{Co}_{22}\text{Ni}_7\text{B}_{19}\text{Si}_5\text{Nb}_4$ ribbons with thickness of 0.07 mm (see Fig. 1)

No.	1	2	3	4	5	6	7	8	9	10
I	1648	874	1120	1197	1413	1413	1524	1413	1413	1314
II	1314	1789	927	1049	1197	1120	1524	1197	1120	1648
III	1049	825	1049	1120	1049	1120	927	985	1049	1197
IV	1049	985	1049	1314	1049	927	985	1314	1314	1049
V	1412	1120	1120	1314	1524	1120	1314	985	1197	1314
VI	1049	1049	1120	1524	1197	1314	1120	985	927	1197

Table 3.

Results of microhardness H_v experiments of $\text{Fe}_{43}\text{Co}_{22}\text{Ni}_7\text{B}_{19}\text{Si}_5\text{Nb}_4$ ribbons with thickness of 0.27 mm (see Fig. 1)

No.	1	2	3	4	5	6	7	8	9	10
I	1049	927	1049	780	825	985	1049	1197	1413	1049
II	1049	985	874	780	874	985	1314	985	927	780
III	1197	1049	985	1049	985	874	1314	1197	874	985
IV	927	1049	874	927	1049	927	1145	825	825	1049
V	874	874	874	825	1145	780	1197	1413	1314	1049
VI	1197	1197	927	1197	1197	1197	874	927	1314	927

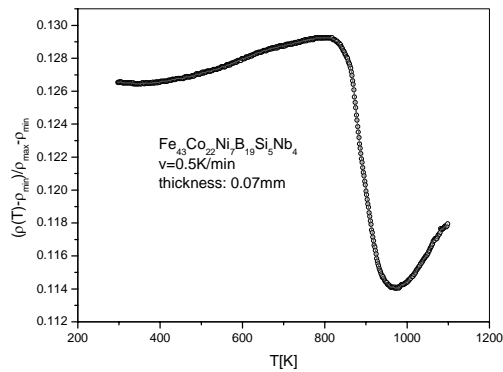


Fig. 5. Normalized isochronous resistivity curves of $\text{Fe}_{43}\text{Co}_{22}\text{Ni}_7\text{B}_{19}\text{Si}_5\text{Nb}_4$ ribbons with thickness of 0.07 mm obtained with heating rate 0.5 K/min

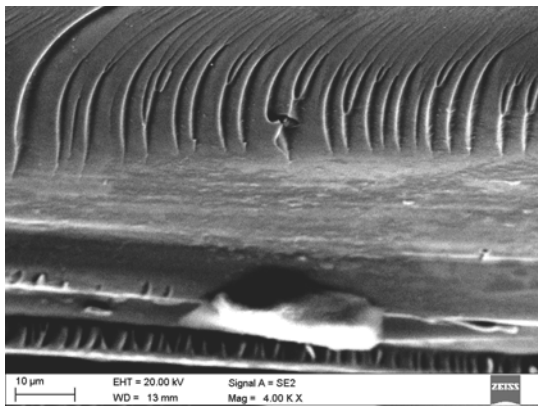


Fig. 6. SEM image of fracture surface of $\text{Fe}_{43}\text{Co}_{22}\text{Ni}_7\text{B}_{19}\text{Si}_5\text{Nb}_4$ ribbons with thickness of 0.07 mm after decohesion; smooth fracture inside with narrow dense veins network in surface having contact with the copper roller during casting and with few veins network in surface freely solidified

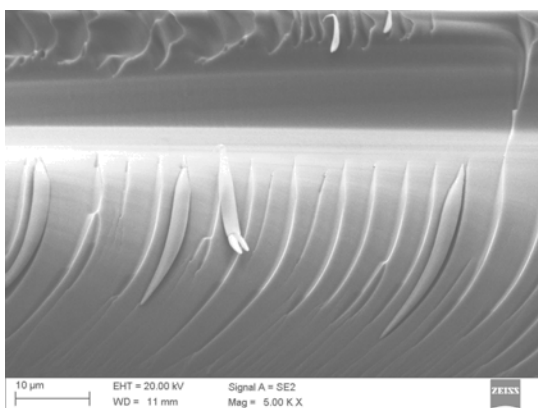


Fig. 7. SEM image of fracture surface of $\text{Fe}_{43}\text{Co}_{22}\text{Ni}_7\text{B}_{19}\text{Si}_5\text{Nb}_4$ ribbons with thickness of 0.27 mm after decohesion; smooth fracture inside with narrow dense veins network in surface having contact with the copper roller during casting and with few veins network in surface freely solidified

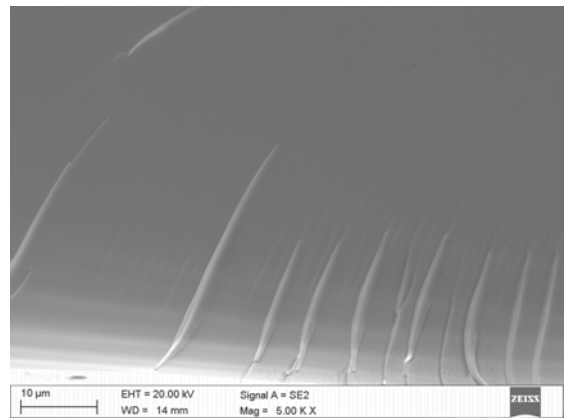


Fig. 8. SEM image of fracture surface of $\text{Fe}_{43}\text{Co}_{22}\text{Ni}_7\text{B}_{19}\text{Si}_5\text{Nb}_4$ ribbons with thickness of 0.27 mm after decohesion; smooth fracture inside with few veins network in surface freely solidified

4. Conclusions

The obtained amorphous ribbons are 10× thicker than classical ribbons (thickness ~0.03 mm).

We can state that the ribbons of $\text{Fe}_{43}\text{Co}_{22}\text{Ni}_7\text{B}_{19}\text{Si}_5\text{Nb}_4$ alloy have an amorphous structure and good soft magnetic properties. Thinner ribbons of $\text{Fe}_{43}\text{Co}_{22}\text{Ni}_7\text{B}_{19}\text{Si}_5\text{Nb}_4$ alloy exhibit better soft magnetic properties than the other ribbon.

The following working hypothesis was assumed: depending on cooling rate of ribbons during casting, the amorphous structure of ribbons is different. The different areas of ribbons (e.g. surface having contact with the copper roller during casting, inside ribbon, surface freely solidified) solidified in different time, thus in different areas of ribbons diversified amorphous structure with different content of the so-called free volume (microvoids) and ordered state are presented. This hypothesis was put forward on the basis of results of fracture morphology of $\text{Fe}_{43}\text{Co}_{22}\text{Ni}_7\text{B}_{19}\text{Si}_5\text{Nb}_4$ ribbons with thickness of both 0.07 mm and 0.27 mm after decohesion and microhardness. Morphology is changing from smooth fracture inside with narrow dense veins network in surface having contact with the copper roller during casting to few veins network in surface freely solidified. Microhardness is variable on width of ribbon and is higher on the margin of ribbons than in centre of $\text{Fe}_{43}\text{Co}_{22}\text{Ni}_7\text{B}_{19}\text{Si}_5\text{Nb}_4$ ribbons.

Further more investigation, for example Mössbauer spectrometry has to be conducted on different thickness of ribbons in order to confirm these conclusions.

The excellent magnetic properties and high value of temperature of crystallization $T_x=800$ K lead us to expect that the Fe-based amorphous alloy is promising for the future applications as new engineering and functional material.

Acknowledgements

This work was supported by Polish Ministry of Science under grant No. 0661/T02/2006/31.

References

- [1] A. Inoue, B.L. Shen, C.T. Chang, Fe- and Co-based bulk glossy alloys with ultrahigh strength of over 4000 MPa, *Intermetallics* 14 (2006) 936-944.
- [2] A. Inoue, B. Shen, A. Takeuchi, Fabrication, properties- and applications of bulk glossy alloys in late transition metal-based systems, *Materials Science and Engineering* 441 (2006) 18-25.
- [3] W.H. Wang, Roles of minor additions in formation and properties of bulk metallic glasses, *Progress in Materials Science* 52 (2007) 540-596.
- [4] A. Inoue, Stabilization of metallic supercooled liquid and bulk amorphous alloys, *Acta Materialia* 48 (2000) 279-306.
- [5] B. Shen, A. Inoue, Superhigh strength and good soft-magnetic properties of (Fe,Co)-B-Si-Nb bulk glassy alloys with high glass-forming ability, *Applied Physics Letters* 85/21 (2004) 4911-4913.
- [6] K.F. Yao, C.Q. Zhang, Fe-based bulk metallic glass with high plasticity, *Applied Physics Letters* 90/6 (2007) 061901.
- [7] Ch. Chang, B. Shen, A. Inoue, FeNi-based bulk glassy alloys with superhigh mechanical strength and excellent soft magnetic properties, *Applied Physics Letters* 89/5 (2006) 051912.
- [8] T. Bitoh, A. Makino, A. Inoue, Origin of low coercivity of Fe-(Al, Ga)-(P, C, B, Si, Ge) bulk glassy alloys, *Materials Transaciton* 44/10 (2003) 2020-2024.
- [9] S. Lesz, R. Nowosielski, B. Kostrubiec, Z. Stokłosa, Crystallization kinetics and magnetic properties of a Co-based amorphous alloy, *Journal of Achievements in Materials and Manufacturing Engineering* 16 (2006) 35-39.
- [10] S. Lesz, R. Nowosielski, A. Zajdel, B. Kostrubiec, Z. Stokłosa, Structure and magnetic properties of the amorphous $\text{Co}_{80}\text{Si}_9\text{B}_{11}$ alloy, *Journal of Achievements in Materials and Manufacturing Engineering* 18 (2006) 155-158.
- [11] R. Nowosielski, R. Babilas, P. Ochcin, Z. Stokłosa, Thermal and magnetic properties of selected Fe-based metallic glasses, *Archives of Materials Science and Engineering* 30/1(2008) 13-16.
- [12] B. Shen, C. Chang, A. Inoue, Formation, ductile deformation behavior and soft – magnetic properties of (Fe, Co, Ni)-B-Si-Nb bulk glassy alloys, *Intermetallics* 15 (2007) 9-16.
- [13] S. Lesz, R. Szewczyk, D. Szewieczek, A. Bieńkowski, The structure and magnetoelastic properties of the Fe-based amorphous alloy with Hf addition, *Journal of Materials Processing Technology* 157-158 (2004) 743-748.
- [14] Polish standard PN – EN ISO 6507 – 1:2007.
- [15] P. Kwapuliński, J. Rasek, Z. Stokłosa, G. Badura, B. Kostrubiec, G. Haneczok, Magnetic and mechanical properties in FeXSIB ($X=\text{Cu,Zr,Co}$) amorphous alloys, *Archives of Materials Science and Engineering* 31/1 (2008) 25-28.